ELSEVIER

Journal of Power Sources 86 (2000) 515–522

JOURNAL OF POWER SOURCES

www.elsevier.com/locate/jpowsour

Modelling the integration of a compact plate steam reformer in a fuel cell system

J. Cunha, J.L.T. Azevedo *

Instituto Superior Técnico, Av. Rovisco Pais, 1049-001 Lisbon Codex, Portugal

Accepted 12 November 1999

Abstract

Fuel cell plant design requires an appropriate integration of components, especially with the fuel processing unit. The integration of a steam reformer for methanol with a polymer electrolyte membrane (PEM) fuel cell plant is examined here. The integration considers the use of the fuel cell anode off gas (AOG) for combustion in order to supply the necessary heat for the reforming reaction. The whole fuel cell plant is considered with simple models for the components that allow sizing of the components and characterisation of their operating conditions. A reformer, based on a plate heat exchanger, is considered with catalytic combustion of the AOG and methanol to supply the required energy. A detailed model for a plate heat exchanger, which considers reactions and heat transfer is used to predict temperature profiles. © 2000 Elsevier Science S.A. All rights reserved.

Keywords: Modelling; Fuel cell plant; Steam reforming; Plate heat exchanger

1. Introduction

For the past 10 years, fuel cells have attracted increasing attention due to concerns about energy efficiency and emission reductions. The use of fuel cell systems has been strongly promoted in Japan and in the United States for medium-scale co-generation plants. Nowadays, this interest has been extended to the smaller scale at the residential level. At the same time, increased interest has arisen for the application of fuel cell systems to automotive propulsion, although there is not yet a clear option on the direct use of hydrogen stored on board or the installation of a hydrogen generation plant on board [1]. The use of hydrogen tanks on board introduces safety requirements but can lead to an effective zero-emission vehicle, while fuel processing on board will generate minor emissions.

The challenge for on board fuel processing is the production of an efficient and compact unit to achieve the demanding targets set out for automotive applications. One of the important targets is the achievement of a short start up time that may lead to the need for the use of energy storage buffers. Initial power can be provided either from energy stored in batteries or from the fuel cell using previously processed reformate gas. In either case, this energy buffer is required for load following since the fuel cell power should be used to provide the base load for the automobile.

To achieve adequate efficiency for hydrogen generation on a small scale, the design should take into account the thermal and physical integration of components. For fuel processing, the main methods are the use of partial oxidation or the use of steam reforming. The first technology has the capability of allowing for greater fuel flexibility while the later leads to higher conversion efficiencies. In both cases, the production of hydrogen also generates carbon monoxide that is not tolerated by the cell catalyst. The elimination of carbon monoxide and other undesirable gas components requires the use of a membrane for separation or a shift reactor or a selective oxidation reactor, all of which increase the system complexity.

For the case of steam reforming, the need for a water supply introduces the consideration of water recovery from the fuel cell off gases. Steam reforming is an endothermic reaction and therefore requires heat from an external source. This can be met by the combustion of off-gas streams from the fuel cell.

The design of a fuel cell system, including the balance of plant components, requires an integration study and,

* Corresponding author. Fax: +351-21-847-55-45; e-mail: toste@navier.ist.utl.pt

PII: S0378-7753(99)00482-6

eventually, a detailed design for components where integration of processes is performed. Two modelling approaches implemented to study the performance of a fuel cell system using steam reforming are described. The first approach is based on simple models for the fuel cell plant components that allow the specification of mass and energy fluxes between the components. The second approach is used to predict the temperature distribution in the specific steam reformer considered.

This work was carried within the scope of the MERCATOX project on the 'Development and evaluation of an integrated methanol reformer and catalytic gas clean-up system for a SPFC vehicle'. This project had the final objective of producing a prototype of an integrated fuel processing unit on a 20-kWe scale. The report is part of the contribution of Instituto Superior Tecnico, which had the responsibility of producing the system modelling. The project coordinator was Welman CJB, who performed the tests on the integrated system, ECN developed the coating technique, tested the reformer and combustion catalysts and prepared the reformer units [2], Loughborough University tested catalysts for the gas clean-up unit (GCU) and prepared the units for the integrated system [3]. Rover prepared a specification for the system and continuously monitored the developments.

2. Modelling the fuel cell plant system

2.1. Basic fuel cell plant configuration

A definition of the fuel cell system and of the steam reformer is obtained by considering a plant model in which the main components are modelled with simplified assumptions. The objective of this model is to analyse the possible integration of different components with respect to their heat demand or heat production. The simplified scheme considered for the polymer electrolyte membrane (PEM) fuel cell system using methanol is presented in Fig. 1.

Global energy balances are performed for the individual components in order to define the gas flow and heat streams in the system. Heat losses from all components except the fuel cell are considered here, with a value of 10% of the heat exchanged in each unit. The main operating parameters of the system are briefly described below for the main components.

- *Cell stack*. Stack efficiency was assumed as 60% [4]. H_2 utilisation factor of 85% and 100% excess air. Pressure: 2 bar. Temperature: 80°C. Electrical load: 20 kWe.
- *GCU*. Pressure: 3 bar. Temperature 130°C. 100% excess air based on the CO and unconverted methanol at the GCU inlet. No variation either for CO or methanol.
- *Reformer*. Pressure: 4 bar. Temperature: 200°C, or otherwise indicated.

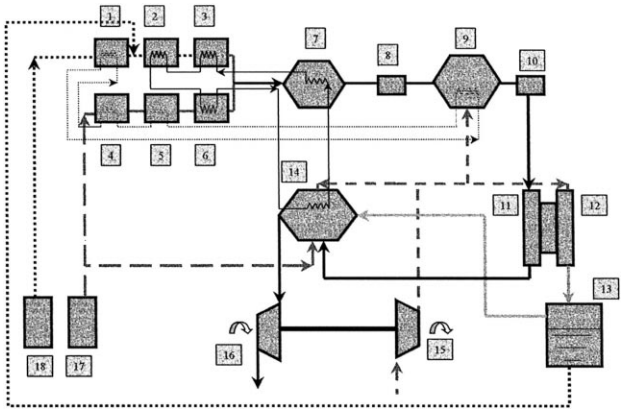

Fig. 1. PEM fuel cell system configuration. (1) Liquid water heater, (2) water evaporation, (3) water super heater, (4) Liquid methanol heater, (5) methanol evaporator, (6) methanol super heater, (7) reformer, (8) heat exchanger, (9) gas cleanup unit, (10) heat exchanger, (11) anode, (12) cathode, (13) water separation, (14) combustion chamber, (15) compressor, (16) turbine, (17) methanol supply, (18) water supply.

- *Combustor*. Pressure: 2 bar. Excess air of 10%, or otherwise indicated.
- Turbine and compressor with isoentropic efficiencies of 70%.

The two off-gas streams from the fuel cell are recycled in the system. From the anode off gas (AOG), there is excess hydrogen available, in a mixture with, mainly, water and carbon dioxide, that can be combusted to supply heat. The remaining gas, stream from the cathode exhaust (CE) has high O_2 content and, therefore, has the option for use as oxidant in the combustor. In either case, the cathode exhaust is assumed to cool and condense the water, allowing its use for the reformer.

Heat exchangers are interposed between the reformer and GCU, and between the GCU and the fuel cell with heat dissipated. The GCU unit has the objective of reducing the CO concentration in the reformate gas to below 10 ppm; the heat produced is used for heating water and methanol and for vaporising methanol.

Water evaporation and water and methanol superheating are considered in separate units. The reformer is modelled by specifying the methanol conversion and operating temperature based on the equilibrium for the water gas shift reaction. For each of these units, the heat demand is calculated from the heat requirement, allowing for 10% of heat loss. The heat is supplied from the combustion of fuel cell off gases and extra air and methanol.

The extra fuel and air required for the combustor are calculated from the heat demand of the reformer and those of the evaporation process not fulfilled by the fuel cell off-gas, and by the heat from the GCU. The extra fuel is assumed to be methanol, while the air required is derived from the compressor. The option of driving the compressor by a turbine is examined, with the inlet temperature for the turbine being fixed at the water saturation temperature plus

50°C. No heat recovery from the turbine exhaust is incorporated.

2.2. Influence of operating conditions and system configuration

Before setting the volumes of the components, simulations were performed to indicate the influence of the main operating conditions and of the system configuration. For this initial calculation, the efficiency of heat exchangers and the conversion efficiency for the reformer are assumed. The reformer conversion has a significant influence on the total system performance; the results shown here correspond to a conversion of 99%.

The efficiency for each condition is evaluated as:

$$\eta_{sys} = \frac{W_e + W_t - W_c}{Q_{in}} \quad (1)$$

where the system work includes the contribution from the turbine (W_t), where appropriate. W_e is the fuel cell electrical work and W_c is the work of the compressor. Q_{in} represents the heat input from methanol, based on the lower heating value (LHV). The pump power is neglected as it represents less than 0.05% of the total power.

These first tests were conducted with two objectives. Firstly, to determine the impact of the component arrangements and integration on the system efficiency, and, secondly, to provide data on heat loads and flow rates for sizing the individual components.

Fig. 2 shows the calculated variation of the system efficiency with steam:carbon ratio (SCR) in the reformer. The efficiency, in general, decreases due to the increased amount of water required, while for the lower SCR, the system efficiency decreases due to the increase in CO from the reformer. The simulations examined five cases.

(1) Case 1, basic system: The system in Fig. 1 was investigated without the use of any of the available heat sources other than the combustion of the AOG, and methanol, when needed. No use of the cathode exhaust was permitted by and all the water required was supplied to the system. The combustion products were not expanded.

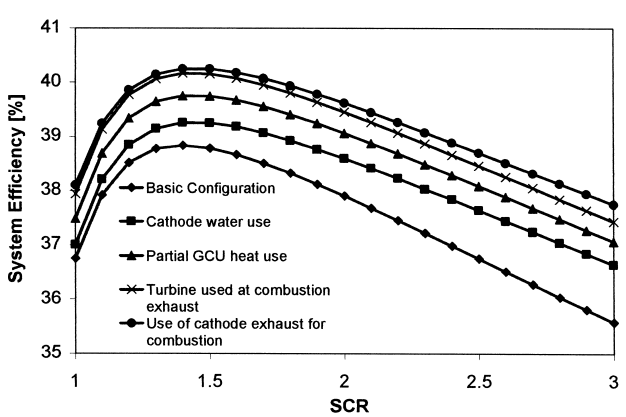

Fig. 2. Fuel cell system efficiency for plant configurations cases 1 to 5.

(2) Case 2: This case corresponds to recycling of the condensed water from the cathode exhaust to the basic system. The gain in efficiency results from the reduction of fuel used for water heating.

(3) Case 3: This case corresponds to case 2, with partial recovery of the GCU heat release. Heat recovery cannot be completed due the operating temperature of the GCU, which is lower than the evaporation temperature.

(4) Case 4: To the configuration of case 3, the expansion of combustion products from a turbine is added. This represents an economy in compression power.

(5) Case 5: This case corresponds to case 4, replacing part of the combustion compressed air by the cathode exhaust after water condensation. This further reduces the compression power requirement.

All these modifications show the capability for increasing system efficiency from a maximum of 37.5% to a value close to 40%. It should be stressed that the total system efficiency is proportional to the fuel cell stack efficiency that was assumed as 60% here.

Integration of components is also used to determine whether the system can be self-sufficient in terms of thermal energy, and in terms of water supply. If the fuel cell off-gas stream is not sufficient to supply the necessary heat input for the reformer, extra methanol for combustion has to be supplied. For the reforming conversion considered, this occurs when lowering the hydrogen utilisation, and when increasing the reformate flow and heat required. The water from the cathode exhaust can meet the demand for the highest conversions and larger hydrogen utilisation factors corresponding to lower reformate flow being required. Those values obviously depend on the SCR and, therefore, for each SCR, the model can be used to define the operating conditions to achieve a self-sufficient system.

2.3. Simplified models for components

The actual performance of the components is determined from their specific characteristics depending on catalyst activity and heat transfer characteristics. Simplified models are formulated and used to calculate the conversion and outlet temperature for each component. The simplified models are also used to size the components and to analyse their operation within the whole system.

The components studied were based on plate finned heat exchangers where the two streams in each component flow into alternating channels. For components where no reaction occurs, the ε-NTU method is used together with correlation for the convection coefficient at the specific surfaces. Uniform temperature is assumed in the vaporiser.

For the reformer components, uniform temperature was assumed and the conversion was calculated from the catalyst reactivity, as a function of temperature, as follows:

$$C = 1 - \exp(-\gamma\tau) \qquad \gamma = k\exp\left(-\frac{E}{RT}\right) \quad (2a\text{–}b)$$

where τ is the residence time that is calculated taking into account the modification of the total number of moles in the reforming process. The reforming catalyst kinetics were defined from specific tests performed in a heat exchanger test unit by ECN [3].

Reforming occurs in a set of channels of the plate finned heat exchanger, the heat being supplied from the catalytic combustion of the fuel cell off-gas streams and additional methanol in the other intermediate channels. The catalytic combustion rates of the AOG and methanol were not assessed in detail, but these reactions are fast and, therefore, an upper limit was set from diffusion between the bulk gas and the catalyst support. The rate thus derived is almost independent of temperature and allows the separate solution of the mass and energy balances for the combustion stream. The mass fuel fraction distribution can be calculated from the inlet value X_0 based on the first-order kinetic rate K, mass flux G and density ρ as a function of the reactor length z:

$$X = X_0 \exp\left(-\frac{K\rho}{G} z\right) \tag{3}$$

to determine the heat release along the length as:

$$\dot{Q} = \dot{Q}_0 \exp\left(-\frac{K\rho}{G} z\right) \text{ with } \dot{Q}_0 = K\rho(\text{LHV})\, X_0 \tag{4a,b}$$

where LHV is the lower heating value from the fuel mixture. Based on this heat release distribution, the temperature profile for the combustion section is calculated from an energy balance accounting for the heat transferred to the alternate stream using a global heat transfer coefficient U and a heat transfer area by volume A_{vol}:

$$Gc_{\text{p}} \frac{\mathrm{d}T}{\mathrm{d}z} = -UA_{\text{vol}}(T - T_{\text{S}}) + Q_0 \exp\left(-\frac{K\rho}{G} z\right). \tag{5}$$

For constant temperature in the alternate stream (T_{S}), this equation can be integrated leading to the temperature profile along the reactor length:

$$T(z) = T_{\text{S}} + (T_0 - T_{\text{S}})\exp(-Bz) + \frac{E}{D-B}(\exp(-Bz) - \exp(-Dz)) \tag{6a}$$

where T_0 is the inlet temperature and

$$B = \frac{UA_{\text{vol}}}{Gc_{\text{p}}} \quad D = \frac{K\rho}{G} \quad E = \frac{K\rho\Delta hX_0}{Gc_{\text{p}}}. \tag{6b,c,d}$$

This simplified model for the temperature distribution in the combustion channels is used to analyse the peak temperature in the components heated by combustion.

2.4. Sizing system components

The implementation of the system in practice is based on the use of pre-selected heat exchangers. Standard off-set fin plate heat exchangers were selected having volumes of 0.5 and 4 l. For the implementation of a prototype, the GCU was designed with a precise temperature control using an external cooling circuit; therefore, this heat requirement was not included in the system. Heating arrangements for methanol were included in the heat exchanger used to cool the reformate, interposed between the reformer and GCU units. The remaining methanol evaporation was accomplished in the unit for steam superheating. Water pre-heating was achieved in the water evaporator.

The sizing of the reformer elements is based on a knowledge of the reforming catalyst activity and on heat transfer characteristics. Fig. 3 presents the reactor volumes calculated as a function of the reformer temperature from the two criteria — reactivity and heat transfer — for three values of conversion: 80%, 90% and 99.9%. All other conditions were kept similar to those for the basic configuration of the system.

Clearly, the dependence of the kinetic rate with temperature is the dominant factor in dimensioning the reformer. Above 250°C, the reformer volume falls below the objective of 10 l desired for conversions in the 90% range. This reforming temperature is higher than the anticipated value of 200°C; the consequences arising will be addressed later. The implementation of the reformer units can thus be achieved using five 4-l units, with 2 l each, for both streams. The volume required from the heat transfer criteria depends on the number of units being considered. An average heat demand for each unit was assumed in order to define the fuel feed flow. For instantaneous combustion, the adiabatic temperature was taken as a conservative value for the inlet and a temperature difference of 20°C was used at the outlet to set the required volume. A more refined temperature distribution, based on Eqs. (6a) and (6b,c,d), was used to specify the fuel staging and component distribution in Section 2.5.

For the other components only, heat transfer criteria were used to size these. Table 1 presents an example of the volumes calculated for the specific case of a SCR = 1.5 with the use of the smaller (0.5 l) or larger (4 l) units. It can be observed that the use of the smaller units (0.5 l) leads to smaller volumes being required due to the increase

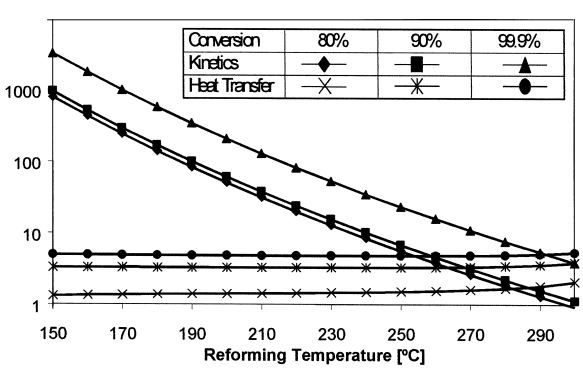

Fig. 3. Required reformer volume in litres as a function of reforming temperature.

Table 1
Calculated volume required for heat exchangers (values are in litre)

ΔT outlet units volume	Water evaporator	Water/ methanol superheater	Ref. cooler methanol heater
100°C/0.5 l	0.5	0.17	0.11
20°C/0.5 l	2.1	0.24	0.11
100°C/4 l	1.2	0.43	0.28
20°C/4 l	5.3	0.61	0.29

of velocity in these units when compared with the larger ones.

Limiting the value of the temperature difference at the heat exchangers outlet ΔT to 20°C, units of 0.5 l were selected for the water and methanol superheater and for the reformate cooler/methanol heater; for the water evaporator, a 4-l unit can be adopted.

2.5. Combustion arrangement

The oxidising stream for combustion is assumed to be in series throughout all the units, with fuel staged feed in each unit to control the heat load and the maximum temperature permitted. Different possibilities exist for the arrangement of components, one of them being illustrated in Fig. 4. The arrangement consists, from top to bottom, of one 4-l HX for water heating and vaporisation of both water and methanol. Next, a 0.5-l unit for superheating the feed to the reformer. The reformer section is comprised of five 4-l units, corresponding to 10-l volumes for the reforming side, and 10 l for combustion. Finally, one 0.5-l unit to cool the reformate for the GCU and heat the liquid methanol before being fed to the vaporiser.

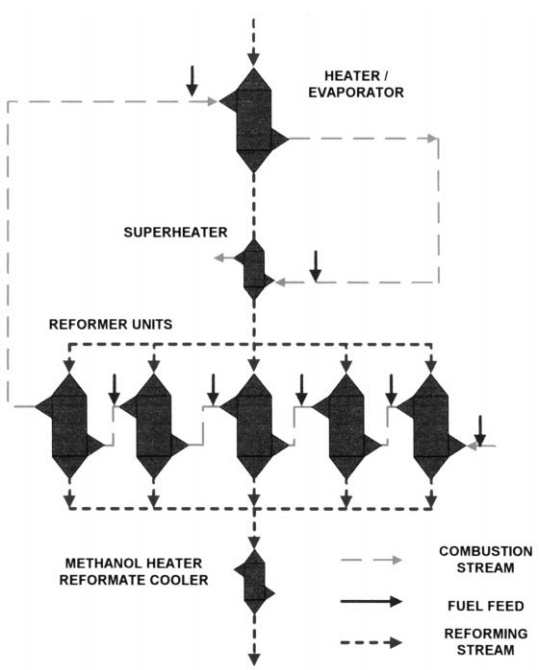

Fig. 4. Arrangement of components for configuration A.

The layout of fuel staging in the units has the objective of meeting local heat requirements by adding the appropriate amount of fuel to the main oxidising gas stream that flows in series through all units. This allows maximum combustion temperatures to be kept within acceptable values. In general, the higher the number of components, the better control can be achieved. The adiabatic temperature provides a conservative estimation criterion for the maximum temperature encountered, while the solution of Eqs. (6a) and (6b,c,d) provides a more realistic value. Based on the geometry and heat transfer characteristics of the heat exchangers, the parameters of Eqs. (6a) and (6b,c,d) were derived and the maximum temperature was estimated based on a constant value for the wall temperature. This wall temperature was taken as 144°C for the evaporator and 173°C for the superheater. For the reformer, a temperature of 250°C was chosen, based on the assumed reactor volume, to achieve a conversion of 90%. The combustion exit temperature from each unit is calculated from Eqs. (6a) and (6b,c,d), and transferred to the inlet of the following unit.

Two configurations were studied. Configuration A corresponds to Fig. 4, where the oxidising stream for combustion is assumed to flow, firstly through the reformer units, and afterwards through the evaporator and superheater. In configuration B, the combustion stream flows firstly into the evaporator followed by the superheater, and then through the reformer. The maximum temperature in the components in the combustion stream are calculated from the temperature distribution in Eqs. (6a) and (6b,c,d). The values obtained are presented in Table 2 for both configurations A and B, and for excess air levels of 10% and 50%. The increase in excess air reduces the peak temperature by increasing the thermal inertia of the oxidiser flow.

The later configuration is found to lead to a higher peak temperature in the evaporator since the total flow rate of oxidant is smaller and has a lower inlet temperature. Configuration A promotes a more uniform set of temperature maxima in each component and further improves the system efficiency as the exhaust gas temperature is decreased. The system efficiency could also be slightly improved by placing the superheater before the evaporator. This would also lead to a decrease in the evaporator peak temperature, but this option was not favoured as the evapo-

Table 2
Calculated peak combustion temperatures [°C] in components

	Excess air 10%			Excess air 50%		
	Evaporator	Sheater	Reformer	Evaporator	Sheater	Reformer
Configuration A	463	350	333	389	316	312
Configuration B	480	369	274	413	333	272

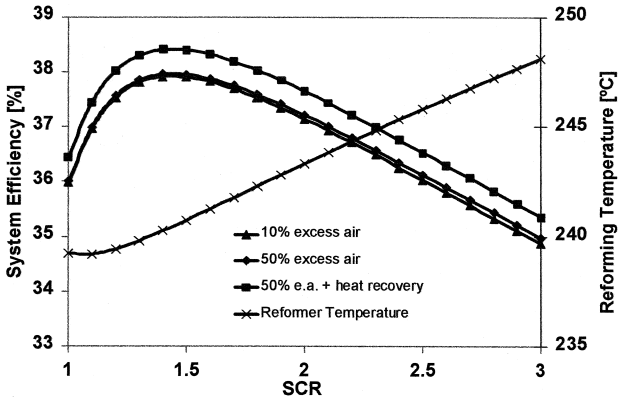

Fig. 5. System efficiency and reformer temperature for the basic configuration, assuming the heat recovery in the reformate cooler is a function of SCR.

rator is easier to assemble with reforming units that have a similar size.

2.6. System performance for the selected components

The definition of a system for testing corresponds to the base configuration, case 1 presented in Section 2.2 with the capability of heating the methanol in the reformate cooler, as considered in Section 2.4. The performance of the components is different from that initially assumed, as they are conditioned by their dimensions, kinetics and heat transfer. For instance, the reformer conversion is coupled with the reformer temperature and volume according to Eq. (2a–b).

The system efficiency is represented in Fig. 5 for the two values of excess air considered in the combustion staging. The figure shows that the increase in excess air from 10% to 50% does not have a large impact on the efficiency. The calculated peak efficiency is lower than for the base case in Fig. 2, due to the increased reformer temperature. When heat recovery is included in the methanol heater/reformate cooler, the system efficiency is increased by about 0.5%. As the reformer temperature is dependent on the reformer dimensions, this value is also indicated in Fig. 5 for 99% reformer conversion. For optimum system efficiency at SCR = 1.5, the reforming temperature is about 240°C.

3. Numerical model of the plate reformer

The fuel cell plant model presented above is an essential step in defining the operating conditions for the reformer. In particular, the definition of the combustion gas composition and staging are important for developing a design for a steam reformer based on a plate heat exchanger construction. This data is necessary to define the input conditions for a numerical model that was developed to allow for the calculation of the temperature profiles within the plates accounting for reaction and heat transfer between the successive plates [5]. The use of this model was found to be of considerable importance in developing the design of a compact steam reformer for natural gas, based on a plate construction [6].

The model calculates the axial profile of mass concentrations for both the reforming and combustion plates, based on kinetic data provided by the user. For both the combustion reforming sections, first-order kinetic rates are assumed for the consumption of the fuel. The reforming products are determined from the equilibrium of the water gas shift reaction. The model can be configured to include any number of plates, and the flow can be either in parallel or in series. For the present application, the reformer is designed with parallel flow, while the combustion flow is in series with staged feed of fuel between the units. Fig. 6 shows a sketch of two possible flow arrangements in the five consecutive units. The direction of the flow in series can either be alternate (Fig. 6a) for a more compact construction or continuous in the same direction (Fig. 6b) with external tubular connections between the units between the locations indicated (1 to 4). In configuration 6a, the combustion gases are in counter-flow in the intermediate units 2 and 4, while in the second configuration 6b, the

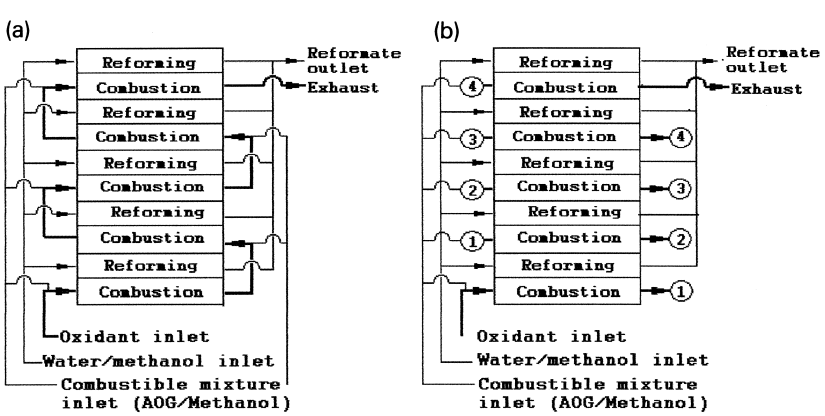

Fig. 6. Arrangement of the flow in the five consecutive units selected for the reformer. (a) Alternate combustion flow, (b) Combustion co-flow in all units.

flow is always in co-flow. The temperature distributions obtained for both of these configurations are presented in Fig. 7, for the case of combustion with 10% excess air. The results for cases 7a and 7b correspond to the configurations in Fig. 6, with the fuel staging distribution calculated from the plant system model. Fig. 7c corresponds to configuration 6a, but with uniform fuel distribution between all the units.

Fig. 7a examines the alternate flow configuration where the temperature profiles for the counter-flow units (2 and 4) can be clearly distinguished from the other units. For the counter-flow situation, the temperature profiles are characterised by a temperature increase from the combustion inlet, from the right side of the figure, promoting heating of the outlet reforming gas. Towards the inlet of the reformer side, the temperature is lower due to the endothermic reforming reaction and the combustion gases are cooled. The combustion gas in the counter-flow channels is heated by the hotter flow from the reformer inlet. For the co-flow units, 1st, 3rd and 5th, the initial increase in combustion temperature is limited by the heat supply to the reforming reaction, where it is more intense, and, therefore, the temperature decay from the reforming side is limited. For this flow configuration, the lowest reforming conversions were obtained in the 3rd and 5th units, where the inlet combustion temperature is lower leading to an overall reformer conversion of 96.7%. From this test, it is interesting to note that the outlet combustion temperature, 224°C from plate 5 in co-flow, is lower than the average reforming stream outlet temperature of 260°C. The model allows integrated analysis of individual units.

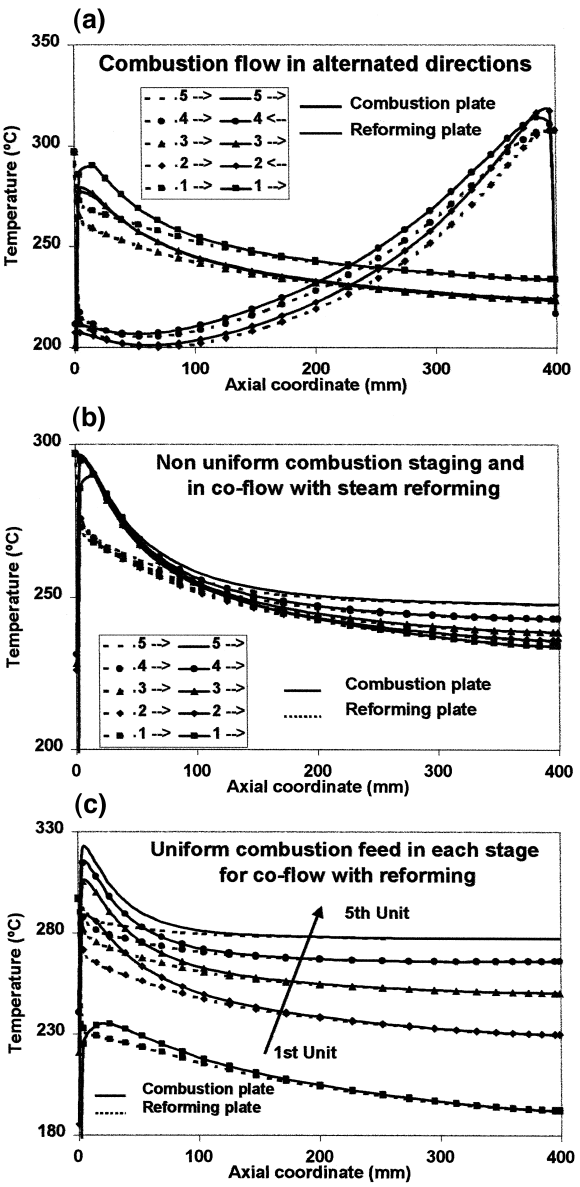

Fig. 7. Calculated temperature distribution with the plate steam reformer numerical model. (a) Alternate combustion flow arrangement. (b) Combustion in co-flow. (c) Combustion in co-flow with uniform fuel staging.

Fig. 7b presents the temperature profiles under co-flow for all the units, as in Fig. 6b, with the non-uniform flow stagging obtained from the plant system model in Section 2.5. All the temperature profiles are similar and the maximum temperature peaks obtained, 300°C, are smaller than the values from the simplified model based on Eqs. (6a) and (6b,c,d). In separate tests, this was confirmed to result from the selection of constant properties from the inlet conditions in the analytical solution. The calculated reforming conversion was 98.4%, a value that is close to the 99% value specified in the plant system model. The small differences between the units are a result of assuming the same staged flow for all the other units except the first, and because the heat losses from the first and last units are slightly larger due to the end plates. The consequence of considering a uniform fuel feed staging in all the units, including the first one, is shown in Fig. 7c. In this case, the energy input in the first unit is not sufficient to achieve the desired temperature, thus, the conversion in this plate is lower. The temperature gradually increases in the other units but the global performance is affected by the poorer performance of the first unit. The average reformer conversion calculated in this case was 91.7% with a reformate outlet temperature of 244°C; the combustion outlet was 277°C for this case.

The numerical model can be applied to show the effects of other parameters, such as the non-uniformity of the flow for the reformers, and the influence of changing the arrangement from five independent units to a fully integrated unit in which the consecutive channels are thermally linked. For this situation, the alternate flow configuration is favoured from a construction point of view, with internal manifolds. The temperature profiles obtained follow the general behaviour shown in Fig. 7a although they are less pronounced due to heat transfer between the co- and counter-flow plates. This model was used to design a compact reformer for natural gas [5]; comparisons were performed with experimental data within that project.

4. Conclusions

A plant model for a PEM fuel cell using methanol is presented and based on realistic assumptions for the components; system efficiencies are estimated as a function of the operating conditions of the fuel cell plant.

Based on the expected operating conditions for the components and on heat transfer characteristics from available heat exchangers, unit sizes were chosen for the main components. Data for reforming kinetics from laboratory tests were incorporated with a target reformer volume of 10 l; the reformer temperature had to be increased to 250°C. The system performance for specific plant components was re-evaluated showing the penalty incurred by the increased reformer temperature and the lower integration.

For implementation of the steam reformer using five available heat exchangers, the staging of the fuel was characterised and the resultant values of flow rates were used in a numerical model for a plate reformer. By adopting co-flow in all the units, good agreement for reformer behaviour was obtained when compared with the chosen specifications. The influence of including other arrangements and staged flow distribution was simulated and discussed showing the capability of the numerical model to evaluate alternative reforming configurations and operating conditions.

Acknowledgements

The work presented was funded by the European Union through the JOE3-CT95-0002 MERCATOX project. Support from this project to J. Cunha and S. Pinheiro, who prepared the numerical model used, is acknowledged. The collaboration of all partners from the MERCATOX project was appreciated and is also acknowledged.

References

[1] S. Dircks, Recent advances in fuel cells for transportation, ISATA Magazine, March 1999, pp. 14–18.
[2] P.J. Wild, M.J.F.M. Verhaak, Third year Technical Progress Report — MERCATOX project. ECN Fuels, Conversion and Environment 7.2020-99/GR1, 1998.
[3] C.D. Dudfield, R. Chen, P.L. Adcock, A compact CO selective oxidation reactor for solid polymer fuel cell powered vehicle application, 6th Groove symposium, London, 13–16 September 1999.
[4] F. Panik, Fuel cells for vehicle applications in cars — bringing the future closer, Journal of Power Sources, 71, pp. 36–38.
[5] S.S. Pinheiro, Modelação numérica de um reactor de placas para reformação catalítica de gás natural, IST Master thesis, 1999 (in Portuguese).
[6] J.L.T. Azevedo, S.S. Pinheiro, Reactor Modelling, Final report for project BRE-CT94-0588, IST, 1997.